scientific reports

Check for updates

OPEN

Early European evidence of artificial cranial modification from the Italian Late Upper Palaeolithic Arene Candide Cave

Tommaso Mori[1,2], Vitale Stefano Sparacello[3], Alessandro Riga[1], Giorgia Ciappi[1], Dario Ferrari[1], Francesca Seghi[4], Fabio Di Vincenzo[5], Monica Zavattaro[2], Filippo Pasquinelli[6], Roberto Carpi[7], Marco Peresani[8,9], Federica Fontana[8], Luca Sineo[10], Jacopo Moggi-Cecchi[1] & Irene Dori[1]✉

This study reports on early Eurasian evidence of artificial cranial modification (ACM) in a Late Upper Palaeolithic (LUP) individual (AC12) from Arene Candide Cave, Italy (ca. 12,620–12,190 Cal BP). We used virtual anthropology and geometric morphometrics to compare AC12's cranial morphology with LUP, Mesolithic, and Neolithic Italian specimens, pathologically modified individuals, and a global sample of ACM cases. Our analyses consistently demonstrate a strong affinity between AC12 and the ACM group, distinct from other comparative samples. Statistical analyses confirm AC12 as a clear outlier for non-ACM groups, with high probabilities of belonging to the ACM cluster. This discovery provides evidence suggesting an earlier origin of ACM on the continent, confirming that this globally distributed practice has Palaeolithic roots. Situated within a complex LUP funerary site, this finding illuminates the deep antiquity of culturally mediated body modification and its role in signifying ascribed identity within ancient hunter-gatherer societies.

Keywords Human body culturalization, Permanent body modifications, Virtual anthropology, Geometric morphometrics

The culturalization of human bodies has been a defining and enduring characteristic of our species. Through transformations in appearance, individuals and societies impart cultural values and symbolic meanings to the physical body, which serves not only as a vessel for personal self-expression but also as a living artifact, moulded by cultural practices and societal beliefs, functioning to convey, uphold, and perpetuate shared values and collective identity (review in[1–3]). For millennia, humans have engaged in a variety of practices, ranging from body adornments to body modifications, to meet cultural standards of beauty and participate in the complex process of creating and reproducing personal, social and ethnic identities (see[4]). The antiquity of these practices is prevalently inferred from findings uncovered at archaeological sites, such as body adornments (e.g., perforated marine shells, beads, pendants, ochre), which can indirectly inform on features such as hairstyles, body paintings, and decorated clothing. This type of evidence has been identified at various sites in Africa and the Mediterranean Levant, dating back to approximately 140,000 years ago (review in[5]).

However, exploring the culturalization of the body in prehistory presents significant challenges, as most forms of body modification are transient. Even modifications regarded as permanent, such as tattoos and piercings, affect only the soft tissues, which are typically not preserved in archaeological remains[3,6]. Tools found in archaeological sites (e.g., "tattoo toolkits") suggest the application of tattoos dates back at least to the Upper

[1]Department of Biology, University of Florence, Florence, Italy. [2]University Museum System, Anthropology and Ethnology Section, University of Florence, Florence, Italy. [3]Department of Life and Environmental Sciences, Neuroscience and Anthropology Section, University of Cagliari, Cagliari, Italy. [4]Department of Cultural Heritage, University of Bologna, Ravenna, Italy. [5]Department of Environmental Biology, Sapienza University of Rome, Rome, Italy. [6]Radiology Unit Firenze 2, San Giovanni di Dio Hospital, Florence, Italy. [7]Imaging Diagnostic Unit Firenze 3, Santa Maria Nuova Hospital, Florence, Italy. [8]Department of Humanities, Prehistoric and Anthropological Science Unit, University of Ferrara, Ferrara, Italy. [9]CNR-Institute of Environmental Geology and Geoengineering, 20126 Milan, Italy. [10]Department of Biological, Chemical and Pharmaceutical Sciences and Technologies, University of Palermo, Palermo, Italy. ✉email: irene.dori@unifi.it

Palaeolithic (18 ka, Mas d'Azil, France[7]), with possibly older but controversial evidence from Blombos Cave, South Africa[8,9]. However, direct evidence of these practices depends on the natural or artificial preservation of human skin. Ötzi, the Tyrolean Iceman discovered in 1991 in the Italian Alps, along with some mummified bodies from Egypt's Predynastic period, exhibit some of the world's oldest preserved tattoos, dating back to the second half of the 4th millennium BCE[10–12]. Skeletal remains provide some of the earliest direct evidence of body modifications, with evidence dating back to the Late Pleistocene. These include nontherapeutic intentional dental modification (review in[13]) and artificial cranial modification (henceforth ACM), also known as intentional cranial deformation (ICD).

The practice involves the application of pressure to an infant's head during its developmental stages, resulting in a reshaping of the cranium. Various instruments used for cranial modifications lead to distinct final shapes[14–21], which can be broadly categorized into two main types (following[14]): tabular modification and circumferential or annular modification. The first type is achieved using rigid objects, such as wooden boards, resulting in a flattening of the occipital and frontal areas and a broadening of the parietal bones. The second type is achieved by using softer tools, such as bandages[20,22], leading to an overall elongation of the neurocranium. The intensity and angles used to shape the heads create different variants within these two main morphological types. Despite the often-fragmentary nature of skeletal remains from archaeological contexts, ACM is documented across various continents and spans millennia, from the end of the Pleistocene to recent times[14–16,23–31].

In this work, we present the evidence of artificial cranial modification in a Late Upper Palaeolithic (henceforth LUP) individual from Arene Candide Cave, in the northwestern coast of Italy (Finale Ligure, Savona, Liguria; Fig. 1a). Arene Candide is one of the most important archaeological prehistoric sites in Europe due to its long occupation spanning from the Upper Palaeolithic to historic times[32–38]. The archaeological and anthropological research in this cave started in the second half of the nineteenth century with the investigation of the Holocene layers[38–41]. In the 1940s, the investigation of the Pleistocene deposits[42–45], uncovered the Epigravettian "necropolis", one of the largest mortuary sites in Europe dated to the LUP in terms of buried individuals (minimum number of individuals: 22[46]). Here, over the course of the Younger Dryas cooling event, generations of hunter-gatherers engaged in a complex funerary program (AMS dates spanning between ca. 12,900 and 11,600 years Cal BP[46]), burying selected individuals and purposefully re-arranging the remains of existing burials—especially crania—around the new depositions[36,45].

Amongst the crania subject to secondary deposition, the one belonging to Arene Candide 12 (henceforth AC12; also known as AC19[47,48]) captivated the interest of Italian scholars due to its peculiar and atypical morphology. The cranium was intentionally placed on the top of another burial (Arene Candide XV, known as "Tomb of the Antlers"), within a niche created by two stone slabs and a broken grindstone (see also[49] for a discussion of the ritual breaking of pebbles at the site), while the mandible and postcranial elements were found in a cluster of bones in secondary deposit nearby (cluster XII[46]; Fig. 1b–d). The skeleton was attributed to an adult male[50]. The first publication of the restored cranium of AC12 (Fig. 1e,f) dates back to the late 1970s, by P. Messeri[48], who after an accurate reconstruction noted its elongated morphology and hypothesized that it represented one of the earliest examples of artificial cranial modification (annular/circumferential oblique type), achieved through constrictive bandaging. However, this interpretation was not supported by Formicola and Scarsini[47], who attributed the extreme cranial morphology to a pathological condition, an accidental event that altered the cranial growth, or the unreliability of the original reconstruction. Comprehensive and detailed information on the biological profile and morphometric description of the cranium, including both the preserved and reconstructed bones, is provided in the works of both authors. The poor quality of collagen extracted from a cranial bone fragment produced an unreliable radiocarbon date, while dates from postcranial elements place AC12 at ca. 12,620–12,190 years Cal BP[46] (95.4% probability; obtained by combining GrM-22237 10,460 ± 40 and GrM-22396 10,465 ± 40, all dates calibrated using OxCal 4.4[51]). Although the calibration curve is quite flat around these dates, resulting in large confidence intervals, the dates from postcranial elements seem consistent with the stratigraphic position of the cranium with respect to the funerary structure of AC 15 (burial XV), whose bones have been directly dated and appear to be slightly younger (GrM-13678 10,325 ± 30, 12,455–11,944 years Cal BP[46], 95.4% probability).

This study employs virtual anthropology and geometric morphometric techniques to quantify the cranial shape of AC12 and explores whether Arene Candide 12 represents early evidence of artificial cranial modification. To do so, we virtually reconstructed the AC12 cranium (henceforth AC12) four times and compared cranial shapes of the virtual reconstructions and the original specimen (henceforth AC12Or) to individuals exhibiting cranial modification, unmodified Italian specimens from the Late Upper Palaeolithic, Mesolithic and Neolithic periods (henceforth LUP-Meso-Neo), as well as individuals with pathological conditions.

Results

Principal component analysis

In our analyses, we used two different landmark sets. The results of the PC1 and PC2 from the first analyses are shown in Fig. 2 (the scatterplot with labels is shown in Supplementary Fig. 3a). PC1 represents 17.51% of total variance. There is no discrimination between groups within this PC1. Maximum positive scores are linked to a rounder and taller frontal bone with an overall shorter neurocranium. Negative PC1 scores are related to a flatter and shorter frontal bone; the neurocranium shows a relatively higher lambdoid region relative to the facial and anterior part of the neurocranium. PC2 represents 12.76% of total variance. This axis differentiates our groups, where negative scores are associated with the pathological and LUP-Meso-Neo crania while positive values are associated mainly with the artificially modified crania. Shapes associated with negative PC2 scores show a flatter occipital area with the nuchal plane more vertical (lambda and opistocranium almost laying on the same plane); the frontal bone and the facial skeleton are also more vertically oriented. Overall, it shows the shape of a short and rounder skull. Positive scores are associated with a long and more flattened cranial shape. In this case, the

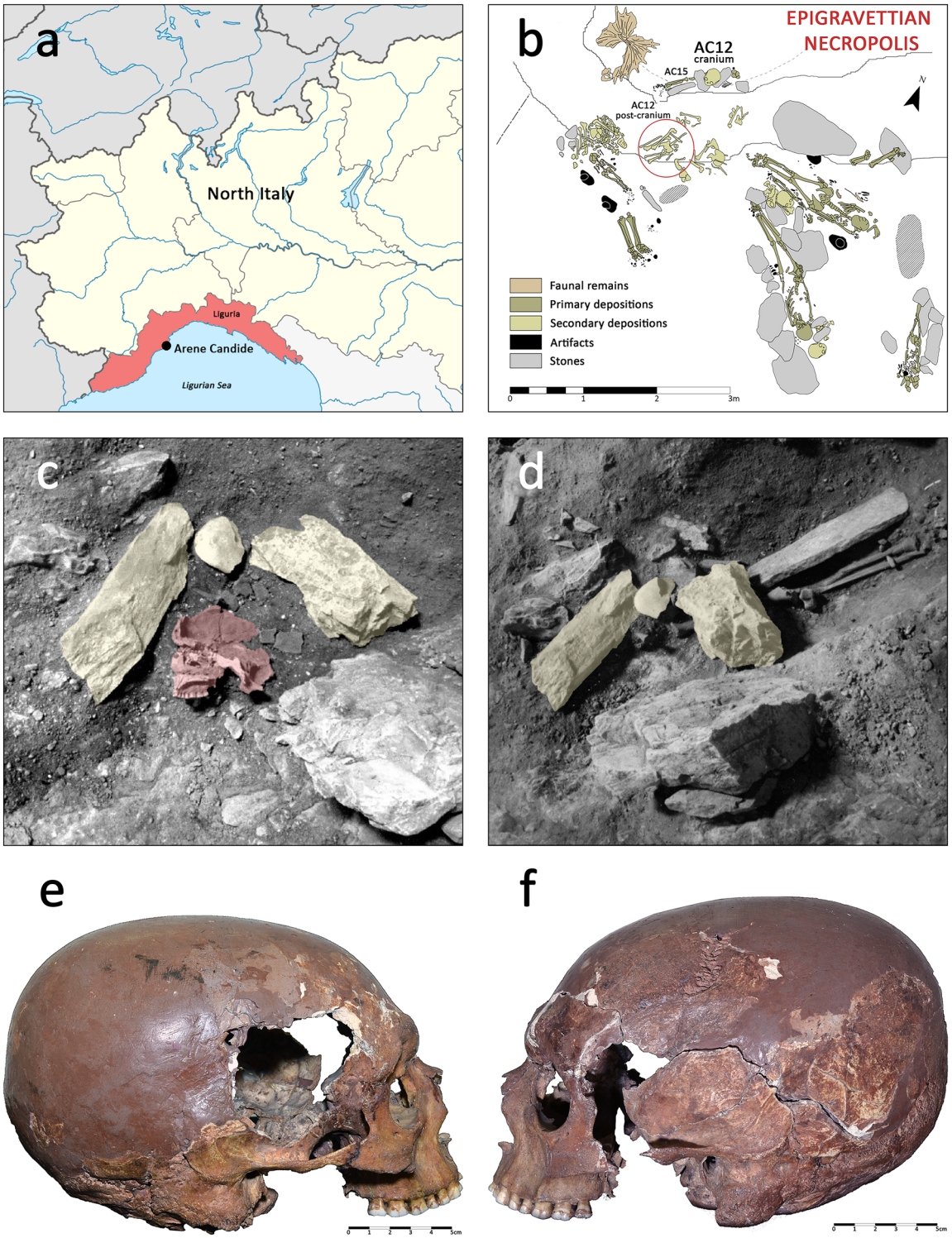

Fig. 1. Location and excavation details of the Arene Candide Cave and AC12 specimen. (**a**) Map of Northern Italy with the location of Arene Candide site; (**b**) The area excavated in the 1940s, later called "Epigravettian necropolis". The AC12 cranium (labelled in a larger font size) and AC12 post-cranial elements (indicated within the red ellipse), along with the AC15 skeleton, are shown in figure. The colours used are explain in the legend; (**c**,**d**) Historical photographs from the original excavation. In (**c**), the cranium (coloured in brown) is located beneath the stones structure (coloured in yellow). In (**d**), the cranium has been removed, and the stones are still in place. The partial excavated AC15 skeleton is clearly visible in the top of right corner; (**e**,**f**) Lateral (left and right) view of AC12 cranium as it is currently preserved in the Museum of Anthropology in Florence.

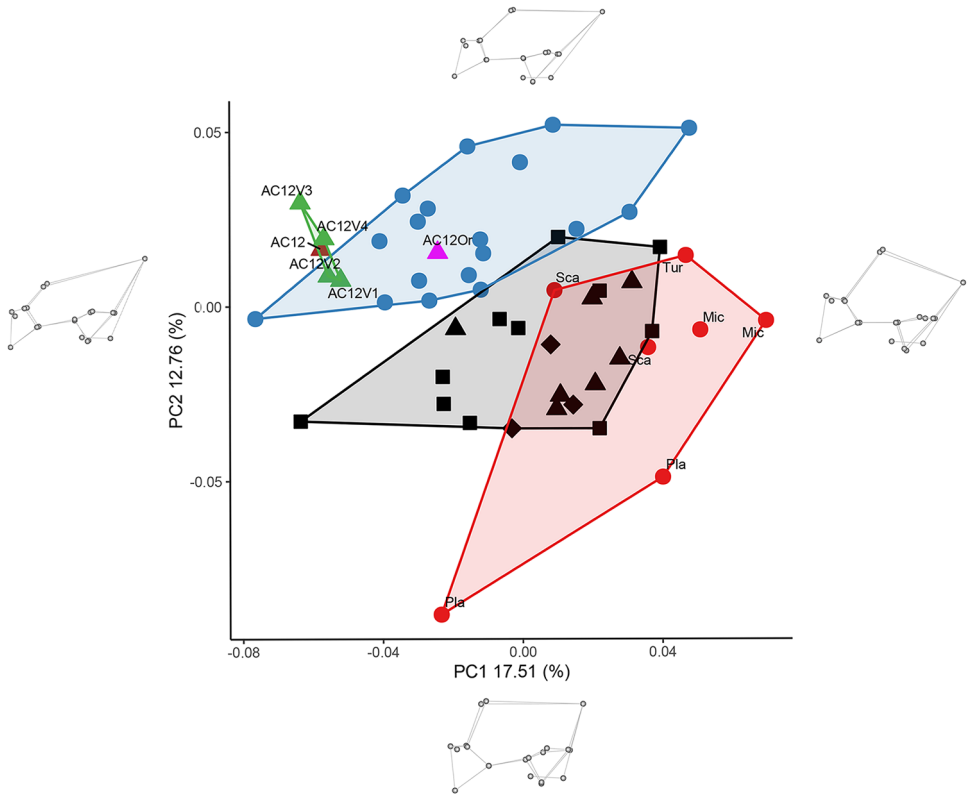

Fig. 2. PC1 and PC2 scatterplot, landmarks analysis. Red circle: pathological or unintentionally modified individuals (Sca: Scaphocefaly, Tur: Turrocephaly, Mic: Microcephaly, Pla: Plagiocephaly). Black triangle: Epigravettian individuals; black square: Neolithic individuals; black diamond Mesolithic individuals. Blue circle: intentionally modified individuals (Annular oblique ACM). Brown triangle: AC12 mean reconstruction; green triangle: different AC12 reconstructions; fuchsia triangle: AC12 original specimen. Shape changes on the sides of the plot exhibit + -2 standard deviation of each PCs, visualized using wireframe in lateral view (left side).

lambdoid region is posteriorly located compared to the foramen magnum. The facial skeleton shows a more prognathic morphology and the frontal bone is flatter and more elongated antero-posteriorly.

In this plot all the reconstructions and the mean configuration of AC12 group close to each other showing similar PC1 and PC2 scores, falling inside or close to the cluster of the annular modified individuals, also AC12Or falls within the ACM cluster with higher PC1 score compared to the virtual reconstructions. The negative PC1 score and positive PC2 score showed by AC12 new reconstructions highlight its elongated and overall flattened morphology. The full results of this PCA—including the PC scores for each individual, eigenvalues, variance explained by each PC, and cumulative variance—are available in the Supplementary_File_Excel_PCA_Sheet1.

The typical probability of AC12 belonging to the three groups based on PC1 and PC2 scores distribution gave p-values below 0.05 if we considered AC12 reconstructions grouped with pathological or LUP-Meso-Neo individuals. Hence, AC12 new reconstructions are considered outliers for these two groups based on PC1 and PC2 scores. Conversely, if we consider AC12 as belonging to the ACM, the typical probability of every reconstruction falls between 0.12 and 0.47 (see Supplementary Table 1 for all p-values calculated). AC12Or typical probability shows similar results with the only exception of p-value for LUP-Meso-Neo group of 0.0537 which is slightly above the alpha level of 0.05.

The second analysis also comprised semilandmarks (Fig. 3, and scatterplot with labels in Supplementary Fig. 3b). In this case, the first PC separates well the modified crania from the other groups. Positive PC1 scores are associated with the ACM group while extreme negative values are reached by the pathological individuals. LUP-Meso-Neo specimens fall in between these two groups. In PC2 groups overlap more but individuals dating from the LUP to the Neolithic period do not reach extreme negative values exhibited by some pathological specimens and artificially modified ones. PC1 represents 31.12% of the total variance; extreme positive values in this component are related to an elongated and flattened morphology. Negative scores are linked to a more pathological shape resembling a scaphocephalic condition (craniosynostosis of the sagittal suture), with a rounder and more vertical frontal bone, and an inferiorly and posteriorly oriented occipital bone. PC2 represents 14.13% of total variance and is associated with a more dolichocephalic shape for positive scores, with a relatively longer neurocranium and a posteriorly projecting occipital bone. Negative scores are linked to a shorter overall calvarium with less round frontal bone and a more oblique nuchal plane.

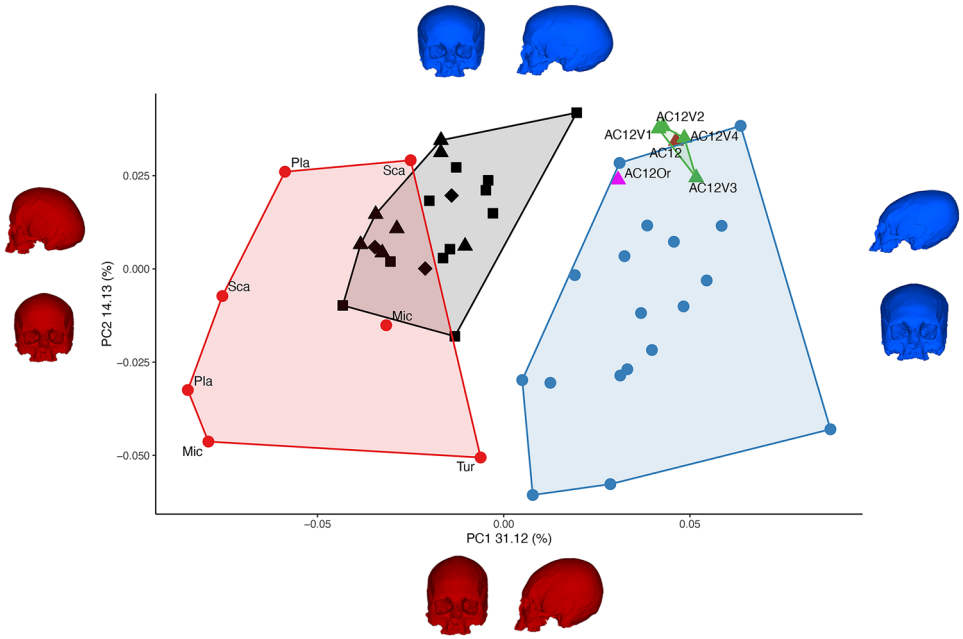

Fig. 3. PC1 and PC2 scatterplot, landmarks and semilandmarks analysis. Red circle: pathological or unintentionally modified individuals (Sca: Scaphocefaly, Tur: Turrocephaly, Mic: Microcephaly, Pla: Plagiocephaly). Black triangle: Epigravettian individuals; black square: Neolithic individuals; black diamond: Mesolithic individuals. Blue circle: intentionally modified individuals (Annular oblique ACM). Brown triangle: AC12 mean reconstruction; green triangle: different AC12 reconstructions; fuchsia triangle: AC12 original specimen. Shape changes on the sides of the plot exhibit + -2 standard deviation of each PCs, visualized using TPS deformation on a reference specimen.

AC12 PC1 and PC2 scores of the different reconstructions and the mean configuration plot together in the proximity or inside the convex hull of the artificially modified individuals. Especially PC1 scores of AC12 fall inside the variability of ACM individuals and outside the variability of the other two groups. AC12 exhibits positive PC2 scores with values on the margin of ACM group variability. AC12Or fall inside the convex hull of ACM individual with lower PC1 and PC2 scores of AC12 mean configuration. The PC1 and PC2 scores of AC12 are linked to an elongated and flatter neurocranial morphology typical of ACM individuals. The full results of this PCA—including the PC scores for each individual, eigenvalues, variance explained by each PC, and cumulative variance—are available in the Supplementary_File_Excel_PCA_Sheet2.

Also, in this analysis, the typical probability of AC12 belonging to the three groups based on PC1 and PC2 scores distribution gave p-values below 0.05 for pathological (range p-values: 0.0003 to 0.0006) or LUP-Meso-Neo groups (range p-values: 0.0081 to 0.0257) while above 0.05 for the ACM group (range p-values: 0.1282 to 0.308) (see Supplementary Table 2 for all p-values calculated). AC12Or follows similar distribution but the p-value of LUP-Meso-Neo group is 0.0735 above the 0.05 alpha level.

Multinomial logistic regression

The Multinomial Principal Component Logistic Regression (MLR) based on the first 6 PCs scores yielded models that correctly classified the comparative sample with an accuracy of 93.48% for the landmarks analysis and 100% for the landmarks and semilandmarks analysis (see Table 1). The first 6 PCs account for 61.43% and 73,75% cumulative variance respectively for the landmarks only and the landmarks and semilandmarks analyses (Supplementary_File_Excel_PCA_Sheet2). In both models all the reconstructions and the original specimen of AC12 indicate a strong morphological affinity to the ACM groups and are all classified in the ACM group (see Table 2).

Pairwise Procrustes distance

When evaluating the overall shape similarities of AC12 with the other individuals' results show that AC12 is more similar on average to the ACM individuals than the other two groups (Fig. 4, blue violin). Interestingly, the Procrustes distances of the LUP-Meso-Neo individuals from AC12 (Fig. 4, grey violin) and the ACM group (Fig. 4, purple violin) have very similar distributions, with almost identical mean values. When considering the Procrustes distance between the different reconstructions (Fig. 4, green violin), the distribution shows a mean value smaller compared with the interindividual Procrustes distance distribution (Fig. 4, yellow violin), which can be referred as normal morphological variability.

	True/predicted	LUP-Meso-Neo	ACM	Pathological
A	LUP-Meso-Neo	20	0	2
	ACM	0	18	0
	Pathological	1	0	5
B	LUP-Meso-Neo	21	0	0
	ACM	0	18	0
	Pathological	0	0	7

Table 1. Confusion matrix of cross-validation results for classification of the different individuals. Lup-Meso-Neo = Late Upper Palaeolithic, Mesolithic and Neolithic individuals. ACM = artificial cranial modification individuals. Pathological = scaphocefaly, turrocephaly, microcephaly, plagiocephaly individuals. A: analysis based on landmarks only; B: analysis based on landmarks and semilandmarks.

		LUP-Meso-Neo	ACM	Pathological
A	AC12 original	$2.93*10^{-4}$	0.99	$3.21*10^{-8}$
	AC12 mean	$2.39*10^{-8}$	1.00	$3.69*10^{-15}$
	AC12V1	$3.42*10^{-5}$	0.99	$9.05*10^{-12}$
	AC12V2	$1.66*10^{-6}$	0.99	$2.62*10^{-13}$
	AC12V3	$4.07*10^{-13}$	1.00	$3.85*10^{-20}$
	AC12V4	$2.04*10^{-8}$	1.00	$5.16*10^{-15}$
B	AC12 original	$4.95*10^{-3}$	0.99	$8.72*10^{-13}$
	AC12 mean	$4.15*10^{-5}$	0.99	$2.59*10^{-17}$
	AC12V1	$1.02*10^{-3}$	0.99	$7.46*10^{-15}$
	AC12V2	$4.09*10^{-4}$	0.99	$5.43*10^{-16}$
	AC12V3	$3.13*10^{-7}$	0.99	$3.99*10^{-21}$
	AC12V4	$1.92*10^{-5}$	0.99	$2.75*10^{-17}$

Table 2. Posterior probability of AC12 classification. LUP-Meso-Neo = Late Upper Palaeolithic, Mesolithic and Neolithic individuals. ACM = artificial cranial modification individuals. Pathological = scaphocefaly, turrocephaly, microcephaly, plagiocephaly individuals. V1, V2, V3, V4 = different reconstructions. A: analysis based on landmarks only; B: analysis based on landmarks and semilandmarks.

Discussion

We analysed four different virtual reconstructions of AC12 and the original physical reconstruction AC12Or using geometric morphometric methods, comparing its cranial shape to a sample of individuals from different Italian sites dating from the LUP to the Neolithic, as well as to pathological or unintentionally modified individuals, and ACM individuals from different regions worldwide. The virtual reconstructions exhibit consistent shapes and consistently cluster within the same region of shape space in both analyses, demonstrating that this critical step was accomplished through a highly reproducible and robust methodology. Given the virtual environment in which the new reconstructions were performed—allowing for semi-automatic alignment of the various fragments—we suggest that the new virtual reconstructions more accurately reflect the original morphology of the fragmented AC12 cranium. All our results confirm strong shape similarities between AC12 and AC12Or to the ACM group. The ACM individuals also show the overall smallest Procrustes distances from AC12. Both the analyses—the more conservative landmarks only and the more comprehensive one using also semilandmarks—show that AC12 exhibits PC1 and PC2 scores consistent with those expected for individuals with artificially modified crania. Classification results based on the first 6 PCs from both analyses also confirm the affinity to the ACM group, with all the reconstructions of AC12 classified into the ACM group. Our results do not support the hypothesis of morphological similarities between AC12 and the LUP-Meso-Neo individuals. The results obtained through geometric morphometric analyses allowed us to test the hypothesis proposed by Formicola and Scarsini[47] that AC12 cranial shape was due to a pathological condition like craniosynostosis, or unintentional modification. Craniosynostosis is the premature fusion of one or more cranial sutures[52], which can occur as spontaneous isolated defects, or may be hereditary or syndromic[53]. The premature closure of a major suture (coronal, metopic, lambdoid, or sagittal) can result in cranial deformity and leads to different cranial shapes, depending on the suture that fuses. AC12 exhibits coronal and lambdoid sutures partially unfused ("significant closure", following[54]). Therefore, the only suture that could have shown synostosis would be the sagittal one, which is not directly observable on AC12. However, pathological individuals with craniosynostosis of the sagittal suture in our sample exhibit cranial shapes that differ from those of AC12 and all the ACM individuals (i.e., the individuals labeled "Sca" in Fig. 3). Early closure of the sagittal suture results in a rounder and more vertical frontal bone, as well as a flatter, posteroinferiorly projecting occipital bone—features absent in AC12 morphology. For these reasons, our results do not support craniosynostosis as a factor influencing the shape of the AC12 cranium.

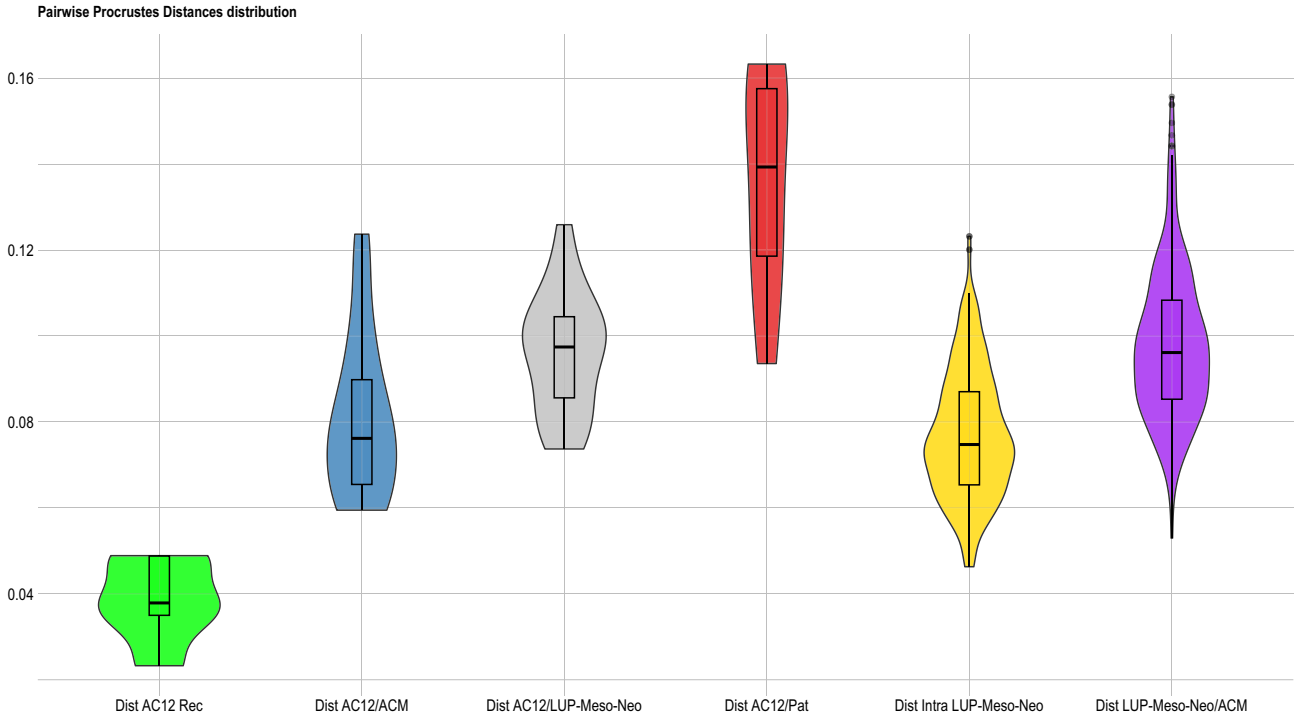

Fig. 4. Violin boxplot of pairwise Procrustes distances (PPD) distributions. Green: PPD between different AC12's reconstructions. Blue: PPD between AC12 mean and ACM individuals. Grey: PPD between AC12 mean and LUP-Meso-Neo individuals. Red: PPD between AC12 mean and pathological individuals. Yellow: interindividual PPD in the LUP-Meso-Neo group. Purple: interindividual PPD between LUP-Meso-Neo individuals.

Having deemed it improbable that craniosynostosis was the cause of AC 12's cranial shape, its attribution to cultural practices seems more plausible. Nonetheless, the cultural shaping of the human body can occur through both direct and indirect means. Many instances of cranial modification documented in archaeological and ethnographic contexts arise from cultural practices that do not deliberately seek to alter the shape of the head, such as positional, postural, or habitual practices (reviewed in[16]). Consequently, distinguishing between intentional and unintentional cranial modifications often proves challenging[16,20,22]. For instance, asymmetrical posterior flattening could result from positioning neonates in a supine position while sleeping to prevent sudden infant death syndrome (SIDS)[55], or from securing children to cradles with bandages or straps for transportation[56]. These changes affect the neurocranium, resulting in asymmetrical (plagiocephaly) or symmetrical (brachycephalic) flattening of its posterior or lateral parts[57,58]. Another habitual practice that could affect the frontal and parietal bones involves the use of tumplines (carrying bands) for occupational purposes. Using headbands to transport heavy objects can flatten the frontal and parietal bones[59] without causing morphological changes in the occipital region. However, the elongated occipital shape observed in AC12 does not support this form of unintentional cranial modification as an explanation.

Results suggest that the cranial shape of AC12 resulted from a cultural practice specifically targeting the head during early infancy, resulting in an annular-type ACM. This would be the earliest known case of artificial cranial modification in Europe, being directly dated to ca. 12,620–12,190 Cal BP[46] (95.4% probability). Currently, the more widely accepted evidence of ACM dates to the terminal Pleistocene or into the Holocene[25,27,60]. The oldest example of ACM in Asia was found amongst prehistoric hunter-gatherers in Northeastern China (Songhuajiang Man I, IVPP PA1683; 9810 ± 30 BP, 11,257–11,192 Cal BP[27], 94.5% probability). Pleistocene evidence of ACM was reported from Southern Australia (Nacurrie I, Murray River region; NZA 1069, 11,440 ± 160 BP[25], 13,738–13,072 Cal BP, 94.5% probability). The idea that ACM was present in the Middle Palaeolithic amongst Neanderthals had been proposed[31,61] but rejected afterwards by the same authors[15,62]. Although the Pleistocene date previously obtained at Nacurrie should be re-performed using modern standards, results from AC12 confirm that ACM has its roots in the Palaeolithic.

In later prehistory, ACM was practiced world-wide, across various cultures and societies for millennia. In the Middle East and Northeast Asia, it continued to be practiced in the Neolithic and beyond[27,63]. In the Eurasian steppes (e.g., Western Asia, Carpathian Basin, Caucasus) ACM is documented from the Bronze Age (3000–1000 BC) to the Medieval Period (5th—fifteenth century AC) with an intensification during the Migration Period of Europe (fourth–seventh century BC)[26,64–67]. In Central and South America, cultural skull modifications were performed for almost 10,000 years, from the Preclassic period to the nineteenth century[14,16,24,28,29,68,69]. Other postmedieval examples of this practice come from Europe, most notably from eighteenth and nineteenth century France[64,70].

Given this ample chronological and geographic spread, it is not surprising that the motivations behind ACM are varied, and in some cases unclear. Explanations for ACM include group identity and kinship, social status, gender roles, spiritual significance, and aesthetic ideals[14,19,20,24,29,69,71]. In some instances, this custom was able to adapt to underlying social changes, evolving, renewing itself, and altering its meaning over centuries[16]. For example, given the unclear reason for the "Toulousienne" head banding custom that was common in rural eighteenth and nineteenth century France, it had been proposed that the focus was primarily the protection of the infant's fontanelles, with the ACM being an unintentional result. However, this has been disputed, given that aesthetic reasons, shared pseudo-medical beliefs, and norms regarding the display of hair and heads were clearly part of the cultural context, which was socially created, transmitted, and reproduced through the manipulation of the infant's head[70]. Indeed, the main difference between ACM and other forms of body modifications—often used as visual markers of significant life events, such as initiation rites, illness, or the loss of a community member (e.g. dental avulsion[72,73])—is that ACM is imposed at birth or shortly afterward and requires a considerable investment of time and effort by parents or caregivers[74,75] (from the first months of life up to five years in some cases). The permanent modification therefore acts as a distinctive visual symbol and a marker of ascribed rather than acquired cultural identity[16,24]. The imposition onto the new-born from the previous generation suggests the presence of inter-generational, long-term transmission of non-negotiable values.

For this reason, ACM is often viewed as an embodiment of hereditary hierarchy, a characteristic typically associated with ranked societies[27]. Indeed, hierarchies were often reinforced by ascribing sacred or supernatural qualities to individuals or groups through the practice of ACM (e.g. the Inca[14], the Maya[29,76], and the Chinookan peoples of the Pacific Northwest[77]), linking appearance to power. However, concluding that the presence of ACM at Arene Candide is evidence of Upper Palaeolithic hierarchical societies would be simplistic. The antiquity of social differentiation along "vertical" lines, particularly within prehistoric hunter-gatherers' societies, is contested (review in[78]). Clark and Neely[79] noted that, while there is substantial evidence of "horizontal" differentiation in archaeological sites across the Europe—stemming from biological sex, age, descendent groups, and recognition earned through individual skills and lifetime achievements—signs of vertical differentiation are less apparent. It has been argued that researchers have often conflated evidence of "complexity" with other characteristics that are typical of Western societies (technological complexity, sedentism, intensification of labour, demographic growth and high population density, hierarchies, etc.)[78]. This obscures the different ways in which prehistoric hunter-gatherers may have been complex, especially in the funerary realm, with more recent approaches exploring possible emphasis on shamanic power, powerful places, horizontal differentiation, and "exceptional people and events"[80–82]. Thus, the evidence of ACM in AC12 does suggest an ascribed identity, but little can be inferred on the nature of power relationships in his group.

Cemeteries are one of the indicators of "complexity" that are often associated to concepts of intensification, territoriality, sedentism, land claim rights, population pressure, and competition for resources[83–85]. While earlier studies linked the appearance of cemeteries with late Mesolithic sedentism and population growth, it is now clear that cemeteries, intended as places set apart for the dead, have Palaeolithic roots[86], with the Epigravettian necropolis of Arene Candide Cave being one of the most notable examples. The site was placed in a highly visible place—a cave on the top of a 90 m white sand dune—and it is conceivable that hunter-gatherers socially invested on this landmark to reinforce their connection to, and privileged access to, an area and its resources[45,87]. In addition, the recent re-assessment of the chronology of the necropolis places it entirely within the Younger Dryas, with the earliest burials dated to its onset, and the last ones to its end, making it reasonable that these territorial claims took place in a context of climatic deterioration[88,89] and increased competition[46,90]. However, compared to modern cemeteries, it is apparent that these Palaeolithic places of the dead were not intended to host the entire group, but only a selected few.

Indeed, it has been observed that Gravettian and Epigravettian burials are rare[87] and include selected individuals, often based on the presence in their skeletal remain of pathological (mostly congenital) deformities, trauma, and other "exceptional people and events"[36,80,82,91]. It has been proposed that, while most dead were treated in other manners[92], formal burial was a means to ritually contain and sanction these "extraordinary" instances. The Epigravettian necropolis at Arene Candide Cave adds an additional layer to this complexity: here, skeletal elements from older depositions, especially crania, were rearranged in relation to new inhumations; in one case, two individuals with similar skeletal deformities were put in relationship through this mortuary gesture[36,46,93,94]. This behaviour evokes a ritual connection between the bones of the ancestors, the newly deceased, and the living individuals performing the funerary rites, as part of a long-term transmission of values and identity continuing over hundreds of years. It is impossible to precisely determine which social role had AC12, with his oddly shaped head, in life and in death. However, his elongated cranium was placed within the covering stones of the burial of AC15, an adolescent showing signs of hypertrophic osteoarthropathy (HOA[95]), which can be a sign of a long-term pulmonary condition or congenital heart disease. Upcoming studies using aDNA will investigate congenital disease and the parental relationships amongst the individuals in the necropolis, providing information on whether AC12 belonged to the same genetic lineage as the Arene Candide Epigravettian group[96]. Currently, the inclusion of AC12 in the funerary program, alongside the deliberate connection with a pathological individual, highlights the exceptional nature of his cranial modifications and underscores its cultural significance within LUP hunter-gatherers at Arene Candide Cave.

In conclusion, AC12 represents the oldest cranium with artificial cranial modification currently documented in Europe, coming from a well-studied and securely dated archaeological context. This finding provides valuable insight into the origins and potential purposes of ACM, although its precise social and cultural significance within past populations, particularly during the Late Upper Palaeolithic, remains difficult to determine. It can be noticed that only one out of the five crania with intact morphology at Arene Candide Cave shows this modification, suggesting that ACM was not an identity marker the entire group, but only of a subset of individuals. Still, as a permanent and highly visible body modification applied during infancy, cranial shaping

symbolizes and physically embodies a trans-generational transmission of ascribed identity. It demonstrates that Upper Palaeolithic human groups perpetuated facets of their cultural identity through diverse practices—extending beyond complex funerary traditions persisting over centuries—many of which remain to be fully uncovered and understood.

Material and methods

The AC12 cranium was physically reconstructed in the 1970s, using plaster to restore missing parts, primarily of the neurocranium (Fig. 1e,f). In light of the concerns expressed by Formicola and Scarsini about the quality of the original reconstruction[47], we opted to perform a virtual reconstruction employing state-of-the-art techniques. To perform a virtual reconstruction AC 12 was CT scanned with Siemens SOMATOM go.TOP (slice thickness = 0.7, pixel size = 0.4748*0.4748, total voxel size = 0.4748*0.4748*0.7 mm). DICOM files were manually segmented using Amira 5.4.5 (Thermo Fisher Scientific). Segmented fragments were saved as separate 3D mesh in .ply format.

The comparative material consists of 46 crania from prehistoric and historic collections, divided into three main groups described below (Table 3). All cranial samples, as well as AC12 specimen, are part of public collections housed in various Italian museums and institutions. The LUP-Meso-Neo sample includes 21 individuals from Italian archaeological sites, primarily stored at the Museo di Storia Naturale of the University of Florence, Museo di Archeologia Ligure in Genova Pegli, and the Museo Archeologico del Finale in Finale Ligure (a complete list of public institutions is provided in Supplementary Table 3). The artificially modified group is made up of 18 individuals, all of them exhibiting clear evidence of the annular oblique type of cranial modification[4,9,11,15,16,19,21,26,45]. These specimens come from different locations and have uncertain chronologies. The pathological group includes 7 individuals with different cranial synostosis, each displaying distinctive morphological characteristic, such as scaphocephaly and turricephaly. All these specimens are part of the historical public collection housed at the Museo di Storia Naturale of the University of Florence. Detailed information on the analysed sample, including the catalogue number, museum facility, archaeological site, geographical provenance, and chronology, is provided in Supplementary Table 3. The 3D models of the specimens were obtained using 3D scanner, photogrammetry, or medical CT scan. The 3D scanner used is the DAVID Structured Light Scanner SLS-3 with a maximum resolution of 0.05 mm and maximum accuracy of 0.05 mm. Photogrammetry was based on pictures shot by a Fujifilm X-T30 with a resolution of 4416*2488 pixels. Photos were then processed in the Agisoft Metashape (v.1.7.6) software. Medical CT-Scan were obtained using a Siemens SOMATOM go.TOP (slice thickness = 0.7, pixel size = 0.4748*0.4748, total voxel size = 0.4748*0.04748*0.7 mm) and saved as DICOM files. DICOM files were opened with Avizo 7.1 (Thermo Fisher Scientific Inc.) and crania were segmented using manual thresholding. The segmented crania were then saved as 3D mesh in .ply format.

Virtual reconstruction of Arene Candide 12

Arene Candide 12 was CT scanned and manually segmented, using Amira 5.4.5, to separate the original bone fragments from the matrix used for the restoration. After segmentation, a total of 4 main fragments were obtained (see Supplementary Fig. 1).

- Almost complete facial skeleton.
- Fragment of left frontal bone articulated with a portion of the parietal bone.
- Right and medial portion of the occipital bone articulated to the right temporal bone.
- Part of the left side of the occipital bone articulated with portions of the left parietal and temporal bones.

Virtual anthropological methods allow to perform reconstruction multiple times. The reconstruction was a necessary and critical part of the analysis. To minimize the uncertainty of the bias introduced by this step, four different reconstructions were performed adopting semi-automatic methods (see below) by three different users (2 times by T.M., one by A.R., and one by I.D.; Supplementary Fig. 2).

We aligned the fragments through a semi-automatic protocol, using the "align" tool in MeshLab[97] software and the *rotmesh.onto()* function from Morpho R package[98].

	M		F		Und. sex			
	Adult	*Sub*	*Adult*	*Sub*	*Adult*	*Sub*		
Group	**n**	**n**	**n**	**n**	**n**	**n**	**tot**	**Geographical provenience of the sample**
ACM	6		6		4	2	18	South America (Argentina n = 2, Peru n = 11) Eurasia (Crimea Peninsula; n = 3) Oceania (Pacific Islands; n = 2)
LUP	5		2					Italy (Ligury n = 15, Veneto n = 2, Sicily; n = 4)
Mesolithic	2		1				21	
Neolithic	6	1	3		1			
Pathological	5		2				7	Italy (Tuscany n = 6) and unknown origin (n = 1)
tot	23	3	13		5	2	46	

Table 3. Comparative sample used in this study. M = male, F = female, Und. sex = undetermined sex; Adu = adult (age class > 20 y.o.), Sub = subadult (age class < 20 y.o.); n = number of specimens for each category.

First, we created a mirrored version of the facial fragment to have a more complete facial skeleton. To align the two parts (original facial portion and mirrored one), we used the align tool in Meshlab. After setting 4 identical points between the two meshes, the software aligned the two elements and performed an iterative cluster point (ICP) algorithm to optimize their position. The aligned mirrored version of the facial skeleton was used to reconstruct the missing left portion of the original ones.

The two fragments of the occipital bone did not have connection points. Instead of aligning the two portions manually, we preferred to create a mirrored version of the right portion and align it to the original right one using the align tool and ICP algorithm in Meshlab. Afterward, we aligned the left portion to the mirrored aligned right one using the same method. The mirrored part was erased leaving only a portion of it that connected the left and right original fragments. To obtain a more complete neurocranium we then performed another mirroring of the achieved reconstruction to reconstruct the missing right parietal portion and the left zygomatic arch using again the align and ICP tool from Meshlab.

The reconstructed facial skeleton and neurocranial part had one portion in direct connection, the zygomatic suture. By collecting four landmarks on the superior and inferior border of the zygomatic suture on the maxilla and temporal bone we used the *rotmesh.onto()* function from the Morpho package[98] to align the two meshes (face and neurocranium).

The last fragment that needed to be aligned was the left fronto-parietal part. In this case, there was no clear evidence of the presence of connecting points between the fragment and the rest of the calvarium. The alignment of this portion was achieved manually using Avizo software 7.1. Once the alignment was performed the overall reconstruction was mirrored again and aligned to the original one using the align and ICP tool in Meshlab to reconstruct the fronto-parietal portion of the right side. The rest of the mirrored mesh was erased leaving only the mirrored version of the fronto-parietal fragment in the correct position (final reconstruction in Fig. 5a,b; Supplementary Fig. 2a–c).

For one of the reconstructions (AC12V1), we estimated also the missing cranial vault. This was done for aesthetic purposes but none of the landmarks or semilandmarks used for the following analysis was taken on this estimated portion. The estimation was achieved using 20 landmarks and 220 semilandmarks placed on AC12V1 and AC5. AC5 was then warped using Thin Plate Spline algorithm[99] on the AC12V1 reconstruction and its vault was kept to reconstruct the missing portion of AC12V1.

To assess the reproducibility and reliability of the reconstructions we calculate the pairwise Procrustes distances among them and compare the distribution of Procrustes distance between the reconstructions with the interindividual distance among the LUP-Meso-Neo group. Moreover, the scores of the first two principal components calculated from the principal component analysis of the different reconstructions will also be evaluated to assess the reliability of this step.

Shape analyses and statistical analyses

We collected a total of 20 common osteometric landmarks (Supplementary Table 4) and 129 surface semilandmarks placed on AC12 neurocranium (Fig. 5c–e). The surface semilandmarks were digitized on one reconstruction of AC12 and used as a patch template. Missing landmarks were estimated through mirroring and Thin Plate Spline (TPS) interpolation, using preserved landmarks[99] for bilaterally missing landmarks. A list of specimens and number of landmarks requiring estimation is provided in Supplementary Table 5. Mirroring was performed using the *fixLMmirror()* function from the Morpho R Package[98], and TPS interpolation was carried out using the *fixTPS()* function from the same package. TPS interpolation estimates missing landmarks based on the five morphologically closest specimens.

The template patch of semilandmarks was projected on the comparative sample using the *placePatch()* function from the Morpho R package[98]. Once placed, the semilandmarks were allowed to slide using the minimum bending energy criterion[100]. The slided semilandmarks were then used for the following analyses. The full raw coordinates of the landmarks and slid semilandmarks are available in the Supplementary_File_CVS_Raw_Coordinates.

We performed two geometric morphometrics (GM) analyses using different datasets. The first is based only on the landmarks configuration and the second adds the surface semilandmarks.

In both analyses we performed Generalized Procrustes Analysis (GPA) in order to translate rotate and scale all landmarks configurations[99,101–103] to produce new Procrustes coordinates, in both analyses, before the GPA, we calculated the mean AC12 configuration and removed all the different versions of AC12 reconstructions leaving in the GPA only the mean AC12 configuration and the AC12Or specimen.

The Procrustes coordinates were analysed using principal component analysis[104] (PCA). In each PCA, we used the covariance matrix built on the comparative sample and AC12 mean reconstruction and the original AC12 specimen configuration. Subsequently, we performed an ordinary Procrustes analysis to register the shapes of the different virtual reconstructions of AC12 on the mean shape of the comparative sample. Lastly, the registered landmark configurations of AC12 reconstructions were projected to predict their principal component (PC) score values. In this way, neither the PCA axes nor the Procrustes coordinates of our reference sample were influenced by the multiple AC12 reconstructions themselves. We explored the PC1 and PC2 scores distribution through scatterplots adding colour and convex hull to the different groups. Shape variation was visualized in two different ways in the two analyses. In the landmarks only, wireframes connecting landmarks were morphed along the major PC axes to visualize how shapes varied along two standard deviations of a given PC axis. Instead, shape changes along PCs in the landmarks and semilandmarks analyses were visualized as a deformation of a 3D surface mesh of a reference specimen (AC IV) based on its landmark configuration transformed via Thin-plate spline interpolation[53] along two standard deviations of a given PC axis.

Based on the PC1 and PC2 scores from both analyses, we computed the typicality probability of AC12 for each group using the *typprobClass()* function from the Morpho R package. This function tests the null hypothesis

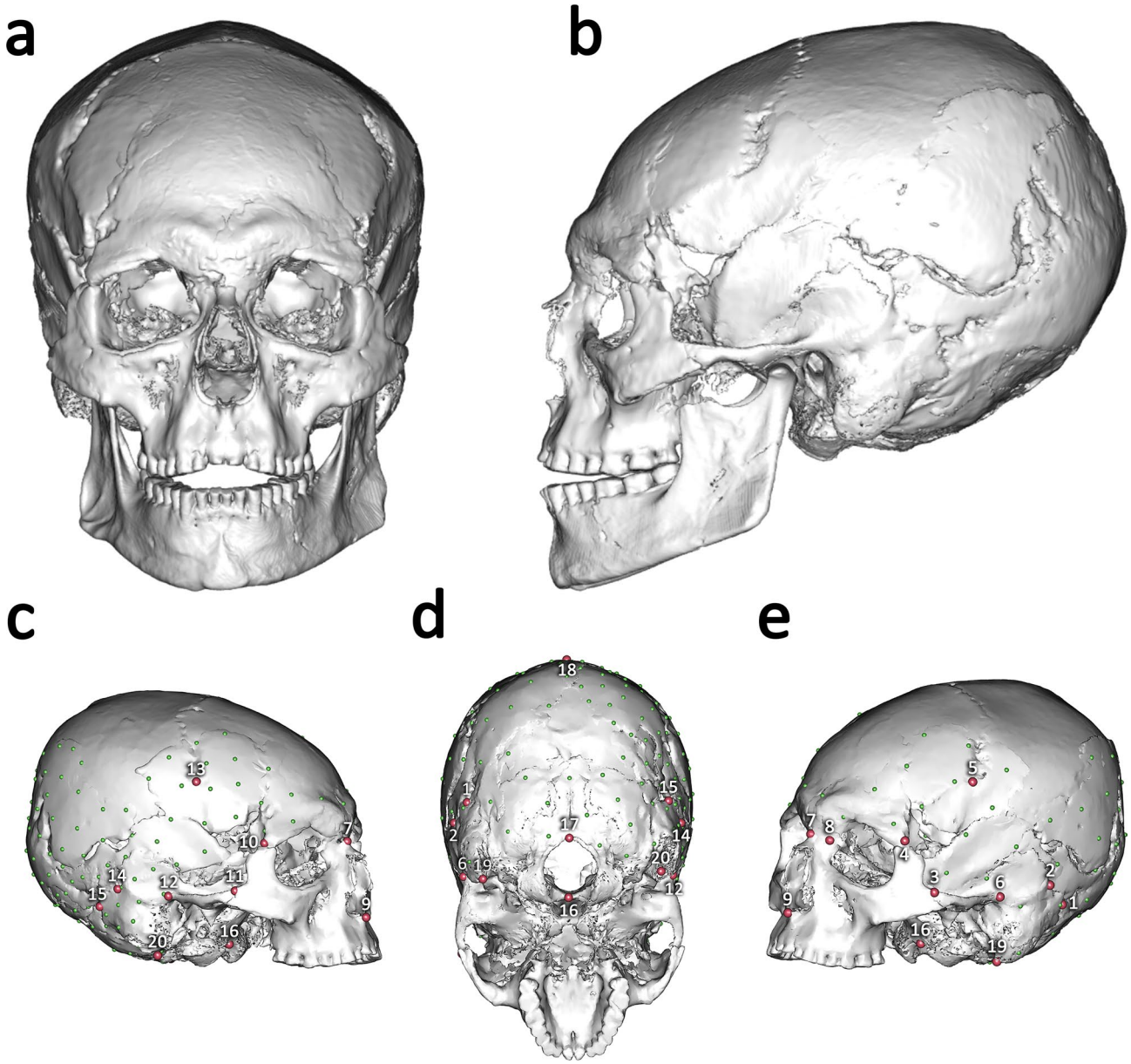

Fig. 5. Virtual reconstruction of AC12 V1 with landmarks and semilandmarks. (**a**,**b**) frontal and left lateral views of full reconstruction of AC12 V1; (**c**–**e**) anterior oblique and inferior views of AC12 V1 showing landmarks (red dots, numbered as listed in Supplementary Table 4) and semilandmarks (small green dots).

that a specimen belongs to a given group, returning a p-value that indicates how typical the specimen is for that group. If the p-value is above the alpha level of 0.05, the null hypothesis cannot be rejected, suggesting the specimen is typical for the group. Conversely, if the p-value is below 0.05, the null hypothesis is rejected, indicating the specimen is atypical and may be considered an outlier. To estimate the morphological affinities and to classify both the reconstructions and the original AC12 specimen into the three defined groups (ACM, LUP-Meso-Neo, pathological), we applied Multinomial Principal Component Logistic Regression (MLR) models[105,106]. These models were based on the principal component (PC) scores obtained from both analyses. The models were constructed using the PC scores of the first six principal components derived exclusively from the comparative sample. The reconstructions and the original specimen were then included a posteriori to estimate their relative affinities to the comparative groups, expressed as percentage probabilities of group membership. The classification accuracy of the model was evaluated through cross-validation of the comparative sample. All analyses were performed using the nnet package[107] (version 7.3–12).

The total shape difference can be evaluated as Procrustes Distance[101,108]. We explored the distribution of pairwise Procrustes distances between AC12 and the members of the three groups, we also measured the pairwise Procrustes distances between all the AC12 reconstruction and the pairwise Procrustes distance between ACM

individuals and LUP, Mesolithic and Neolithic individuals. The distribution of the distances was visualized as a violin box plot.

Data availability

All data that support our results are provided in the Supplementary_File_Excel_PCA and Supplementary_File_CVS_Raw_Coordinates. The 3D surface models of the Palaeolithic Ligurian sample are available online in the MorphoSource project "The Arene Candide 3D Database" https://www.morphosource.org/projects/00000C206?locale=en. The 3D surface models of the other individuals used in this study are available upon request from the host institutions.

Permission statement Permission to study the archaeological skeletal materials was granted by the relevant Superintendency for Archaeological Heritage, as well as by the Museums and Institutions hosting the collections (Soprintendenza Archeologia Belle Arti e Paesaggio per le province di Imperia e Savona; Museo di Storia Naturale di Firenze, Sezione di Antropologia e Etnologia, Università di Firenze, Firenze; Museo di Archeologia Ligure, Genova Pegli; Museo di Archeologia del Finalese, Finale Ligure, Savona; Museo Navale Romano di Albenga, Albenga, Savona; Museo G.G. Gemmellaro, Università di Palermo, Palermo; University of Ferrara, Ferrara; Museo Vittorino Cazzetta, Selva di Cadore, Belluno).

Received: 23 January 2025; Accepted: 24 July 2025
Published online: 30 July 2025

References

1. Manni, F. & d'Errico, F. (eds) *The Oxford Handbook of the Archaeology and Anthropology of Body Modification* (Oxford University Press, 2023). https://doi.org/10.1093/oxfordhb/9780197572528.001.0001.
2. Collins, B. & Nowell, A. (eds) *Culturing the Body: Past Perspectives on Identity and Sociality* (Berghahn Books, 2024). https://doi.org/10.3167/9781805394600.
3. Sofaer, J. R. *The Body as Material Culture: A Theoretical Osteoarchaeology* (Cambridge University Press, 2006). https://doi.org/10.1017/CBO9780511816666.
4. DeMello, M. *Encyclopedia of Body Adornment* (Bloomsbury Publishing, 2007).
5. d'Errico, F., van Niekerk, K. L., Geis, L. & Henshilwood, C. S. New Blombos Cave evidence supports a multistep evolutionary scenario for the culturalization of the human body. *J. Hum. Evol.* **184**, 103438 (2023).
6. Nowell, A. & Cooke, A. Culturing the Paleolithic body: archaeological signatures of adornment and body modification. In *Oxford Handbook of Human Symbolic Evolution* (eds Gontier, N. et al.) 400–428 (Oxford University Press, 2021). https://doi.org/10.1093/oxfordhb/9780198813781.013.20.
7. Péquart, S.-J. & Péquart, M. L. N. Grotte du Mas d'Azil (Ariège): une Nouvelle Galerie Magdalénienne. *An. Paléontol.* **XLVI**, 127–194 (1960).
8. Deter-Wolf, A. The material culture and middle stone age origins of ancient tattooing. In *Tattoos and Body Modifications in Antiquity* (eds Della Casa, P. & Witt, C.) 15–26 (Chronos Verlag, 2013).
9. Henshilwood, C. S. et al. A 100,000-year-old ochre-processing workshop at Blombos Cave, South Africa. *Science* **334**, 219–222. https://doi.org/10.1126/science.1211535 (2011).
10. Deter-Wolf, A., Robitaille, B., Krutak, L. & Galliot, S. The world's oldest tattoos. *J. Archaeol. Sci. Rep.* **5**, 19–24. https://doi.org/10.1016/j.jasrep.2015.11.007 (2016).
11. Deter-Wolf, A., Robitaille, B., Riday, D., Burlot, A. & Jacobsen, M. S. Chalcolithic tattooing: historical and experimental evaluation of the Tyrolean Iceman's body markings. *Eur. J. Archaeol.* **27**, 267–288. https://doi.org/10.1017/eaa.2024.5 (2024).
12. Friedman, R. et al. Natural mummies from Predynastic Egypt reveal the world's earliest figural tattoos. *J. Archaeol. Sci.* **92**, 116–125. https://doi.org/10.1016/j.jas.2018.02.002 (2018).
13. Burnett, S. E. & Irish, J. D. *A World View of Bioculturally Modified Teeth* (University Press of Florida, 2017).
14. Andrushko, V. A. Revelations of ancient head shape: Cranial modification in the Cuzco region of Peru, Early Horizon to Inca Imperial Period. *Am. J. Phys. Anthropol.* **175**, 95–105. https://doi.org/10.1002/ajpa.24201 (2021).
15. Clark, J. L. et al. Identifying artificially deformed crania. *Int. J. Osteoarchaeol.* **17**, 596–607. https://doi.org/10.1002/oa.910 (2007).
16. Tiesler, V. *The Bioarchaeology of Artificial Cranial Modifications: New Approaches to Head Shaping and its Meanings in Pre-Columbian Mesoamerica and Beyond* (Springer, 2013).
17. Anton, S. C. Intentional cranial vault deformation and induced changes of the cranial base and face. *Am. J. Phys. Anthropol.* **79**, 253–267. https://doi.org/10.1002/ajpa.1330790213 (1989).
18. Dingwall, E. J. *Artificial Cranial Deformation: a Contribution to the Study of Ethnic Mutilations* (John Bale, Sons & Danielsson Ltd, 1931).
19. Imbelloni, J. Los pueblos deformadores de los Andes: La deformación intencional de la cabeza como arte y como elemento diagnóstico de las culturas. *An. Mus. Hist. Nat. Bernardino Rivadavia* **37**, 209–254 (1933).
20. Tiesler, V. An introduction to artificial cranial vault modifications. In *The Oxford Handbook of the Archaeology and Anthropology of Body Modification* (eds Manni, F. & d'Errico, F.) (Oxford University Press, 2024). https://doi.org/10.1093/oxfordhb/9780197572528.013.11.
21. Gerszten, P. C. An investigation into the practice of cranial deformation among the Pre-Columbian peoples of northern Chile. *Int. J. Osteoarchaeol.* **3**, 87–98. https://doi.org/10.1002/oa.1390030205 (1993).
22. Torres-Rouff, C. Cranial modification and the shapes of heads across the Andes. *Int. J. Paleopathol.* **29**, 94–101. https://doi.org/10.1016/j.ijpp.2019.06.007 (2020).
23. Antón, S. C. Cranial growth in Homo erectus: how credible are the Ngandong juveniles?. *Am. J. Phys. Anthropol.* **108**, 223–236. https://doi.org/10.1002/(SICI)1096-8644(199902)108:2%3c223::AID-AJPA7%3e3.0.CO;2-8 (1999).
24. Blom, D. E. Embodying borders: human body modification and diversity in Tiwanaku society. *J. Anthrop. Archaeol.* **24**, 1–24. https://doi.org/10.1016/j.jaa.2004.10.001 (2005).
25. Brown, P. Nacurrie 1: Mark of ancient Java, or a caring mother's hands, in terminal Pleistocene Australia?. *J. Hum. Evol.* **59**, 168–187. https://doi.org/10.1016/j.jhevol.2010.05.007 (2010).
26. McKenzie, H. G. & Popov, A. N. A metric assessment of evidence for artificial cranial modification at the Boisman 2 Neolithic cemetery (ca 5800–5400 14C BP), Primorye, Russian Far East. *Quat. Int.* **405**, 210–221. https://doi.org/10.1016/j.quaint.2015.06.007 (2016).
27. Ni, X. et al. Earliest-known intentionally deformed human cranium from Asia. *Archaeol. Anthropol. Sci.* **12**, 93. https://doi.org/10.1007/s12520-020-01045-x (2020).
28. Perez, S. I. Artificial cranial deformation in South America: a geometric morphometric approximation. *J. Archaeol. Sci.* **34**, 1649–1658. https://doi.org/10.1016/j.jas.2006.12.003 (2007).

29. Tiesler, V. Studying cranial vault modifications in ancient Mesoamerica. *J. Anthropol. Sci.* **90**, 33–58. https://doi.org/10.4436/jass.90007 (2012).
30. Zhang, Q. et al. Intentional cranial modification from the Houtaomuga Site in Jilin, China: Earliest evidence and longest in situ practice during the Neolithic Age. *Am. J. Phys. Anthropol.* **169**, 747–756. https://doi.org/10.1002/ajpa.23888 (2019).
31. Trinkaus, E. Artificial cranial deformation in the Shanidar 1 and 5 Neandertals. *Curr. Anthrop.* **23**, 198–199 (1982).
32. Arobba, D., Panelli, C., Caramiello, R., Gabriele, M. & Maggi, R. Cereal remains, plant impressions and 14C direct dating from the Neolithic pottery of Arene Candide Cave (Finale Ligure, NW Italy). *J. Archaeol. Sci. Rep.* **12**, 395–404. https://doi.org/10.1016/j.jasrep.2017.02.015 (2017).
33. Del Lucchese, A. The Neolithic burials from Arene Candide: the Bernabò Brea-Cardini excavation. In *Arene Candide: A Functional and Environmental Assessment of the Holocene Sequence (Excavations Bernabò Brea-Cardini 1940–1950)* (eds Maggi, R. et al.) *Mem. Ist. Ita Paleontol. Um.,* Vol. 5, 605–609 (1997).
34. Formicola, V., Pettitt, P. B., Maggi, R. & Hedges, R. Tempo and mode of formation of the Late Epigravettian necropolis of Arene Candide cave (Italy): direct radiocarbon evidence. *J. Archaeol. Sci.* **32**, 1598–1602. https://doi.org/10.1016/j.jas.2005.04.013 (2005).
35. Sparacello, V. S. et al. Dating the funerary use of caves in Liguria (northwestern Italy) from the Neolithic to historic times: Results from a large-scale AMS campaign on human skeletal series. *Quat. Int.* **536**, 30–44. https://doi.org/10.1016/j.quaint.2019.11.034 (2020).
36. Sparacello, V. S. et al. New insights on Final Epigravettian funerary behaviour at Arene Candide Cave (Western Liguria, Italy) from osteological and spatial analysis of secondary bone deposits. *J. Anthropol. Sci.* **96**, 161–184. https://doi.org/10.4436/JASS.96003 (2018).
37. Bietti, A. & Molari, C. The Upper Pleistocene deposit of the Arene Candide cave (Savona, Italy): general introduction and stratigraphy. *Quat. Nova* **4**, 9–27 (1994).
38. Maggi, R. Summary: a modern excavation carried out fifty years ago. In *Arene Candide: A Functional and Environmental Assessment of the Holocene Sequence (Excavations Bernabò Brea-Cardini 1940–1950)* (eds. Maggi, R. et al.) *Mem. Ist. Ita Paleontol. Um.* **5**, 635–642 (1997).
39. Issel, A. D. una caverna ossifera di Finale. *Atti Soc. Ita. Sci. Nat.* **7**, 173–185 (1864).
40. Issel, A. Liguria Preistorica, vol. XL. *Atti Soc. Lig. Storia Patria* (1908).
41. Rossi, S., Panelli, C., De Pascale, A. & Maggi, R. Di una caverna ossifera di Finale: Evidenze di archeologia ottocentesca nella Caverna delle Arene Candide. In *150 anni di preistoria e protostoria in Italia, Studi di preistoria e protostoria,* Vol. 1, 239–246 (2014).
42. Cardini, L. Nuovi documenti sull'antichità dell'uomo in Italia: reperto umano del Paleolitico superiore nella Grotta delle Arene Candide. *Raz. Civil.* **3**, 5–25 (1942).
43. Cardini, L. Gli strati mesolitici e paleolitici della Caverna delle Arene Candide. *Riv. Stu. Lig.* **12**, 29–37 (1947).
44. Cardini, L. L. necropoli mesolitica delle Arene Candide (Liguria). *Mem. Ist. Ita. Paleontol. Um.* **3**, 9–31 (1980).
45. Riel-Salvatore, J. et al. New insight into the Paleolithic chronology and funerary ritual of Cavena delle Arene Candide. In *Palaeolithic Italy: Advanced Studies on Early Human Adaptation in the Apennine Peninsula* (eds Borgia, V. & Cristiani, E.) 335–355 (Sidestone Press, 2018).
46. Sparacello, V. S. et al. New human remains from the Late Epigravettian necropolis of Arene Candide (Liguria, northwestern Italy): Direct radiocarbon evidence and inferences on the funerary use of the cave during the Younger Dryas. *Quat. Sci. Rev.* **268**, 107131. https://doi.org/10.1016/j.quascirev.2021.107131 (2021).
47. Formicola, V. & Scarsini, C. Contribution to the knowledge of the late Epigravettian human remains from Arene Candide cave (Liguria, Italy): A peculiar-shaped skull. *Homo (Stuttgart)* **38**, 160–170 (1987).
48. Messeri, P. Un cranio mesolitico ligure intenzionalmente deformato alle Arene Candide nel Finalese. *Arch. Antrop. Etn.* **109**, 497–510 (1979).
49. Gravel-Miguel, C., Riel-Salvatore, J., Maggi, R., Martino, G. & Barton, C. M. The breaking of ochred pebble tools as part of funerary ritual in the Arene Candide epigravettian cemetery. *Camb. Archaeol. J.* **27**, 331–350. https://doi.org/10.1017/S0959774316000640 (2017).
50. Paoli, G., Parenti, R. & Sergi, S. Gli scheletri mesolitici della caverna delle Arene Candide (Liguria). *Mem. Ist. Ita. Paleontol. Um.* **3**, 31–154 (1980).
51. Bronk Ramsey, C. Bayesian analysis of radiocarbon dates. *Radiocarbon* **51**, 337–360. https://doi.org/10.1017/S0033822200033865 (2009).
52. Governale, L. S. Craniosynostosis. *Pediatr. Neurol.* **53**, 394–401. https://doi.org/10.1016/j.pediatrneurol.2015.07.006 (2015).
53. Lajeunie, E., Crimmins, D. W., Arnaud, E. & Renier, D. Genetic considerations in nonsyndromic midline craniosynostoses: a study of twins and their families. *J. Neurosurg. Pediatr.* **103**, 353–356. https://doi.org/10.3171/ped.2005.103.4.0353 (2005).
54. Meindl, R. S. & Lovejoy, C. O. Ectocranial suture closure: A revised method for the determination of skeletal age at death based on the lateral-anterior sutures. *Am. J. Phys. Anthropol.* **68**, 57–66. https://doi.org/10.1002/ajpa.1330680106 (1985).
55. Argenta, L. C., David, L. R., Wilson, J. A. & Bell, W. O. An increase in infant cranial deformity with supine sleeping position. *J. Craniofac. Surg.* **7**, 5–11. https://doi.org/10.1097/00001665-199601000-00005 (1996).
56. Dembo, A. & Imbelloni, J. *Deformaciones Intencionales del Cuerpo Humano de Carácter Étnico* (Humanior, 1938).
57. Hutchison, B. L., Hutchison, L. A., Thompson, J. M. & Mitchell, E. A. Plagiocephaly and brachycephaly in the first two years of life: a prospective cohort study. *Pediatrics* **114**, 970–980. https://doi.org/10.1542/peds.2003-0668-f (2004).
58. Rogers, G. F. Deformational plagiocephaly, brachycephaly, and scaphocephaly. Part I: terminology, diagnosis, and etiopathogenesis. *J. Craniofac. Surg.* **22**, 9–16. https://doi.org/10.1097/scs.0b013e3181f6c313 (2011).
59. Gervais, V. E. uso del mecapal en Guatemala y sus consecuencias sobre la columna cervical (primeras observaciones). *Estudios Antropol. Biol.* https://doi.org/10.22201/iia.14055066p.2010.43089 (2001).
60. Solecki, R. S., Solecki, R. L. & Agelarakis, A. P. *The Proto-Neolithic Cemetery in Shanidar Cave* (Texas A&M University Press, 2004).
61. Weidenreich, F. On the earliest representatives of modern mankind recovered from the soil of east Asia. *Pek. Nat. Hist. Bul.* **13**, 161–174 (1939).
62. Chech, M., Groves, C. P., Thorne, A. & Trinkaus, E. A new reconstruction of the Shanidar 5 cranium. *Paléorient* **25**, 143–146 (1999).
63. Fletcher, A., Pearson, J. & Ambers, J. The manipulation of social and physical identity in the pre-pottery Neolithic: Radiographic evidence for cranial modification at Jericho and its implications for the plastering of skulls. *Camb. Archaeol. J.* **18**, 309–325. https://doi.org/10.1017/S0959774308000383 (2008).
64. Galiay, L. et al. Intentional craniofacial remodelling in Europe in the XIXth century: Quantitative evidence of soft tissue modifications from Toulouse, France. *J. Stomatol. Oral Maxillofac. Surg.* **123**, e342–e348. https://doi.org/10.1016/j.jormas.2022.05.002 (2022).
65. Kiszely, I. *The Origins of Artificial Cranial Formation in Eurasia from the Sixth Millennium BC to the Seventh Century AD* (BAR Publishing, 1978).
66. Mayall, P. & Pilbrow, V. A review of the practice of intentional cranial modification in Eurasia during the Migration Period (4th–7th c AD). *J. Archaeol. Sci.* **105**, 19–30. https://doi.org/10.1016/j.jas.2018.12.007 (2019).

67. Torres-Rouff, C. & Yablonsky, L. T. Cranial vault modification as a cultural artifact: a comparison of the Eurasian steppes and the Andes. *Homo* **56**, 1–16. https://doi.org/10.1016/j.jchb.2004.09.001 (2005).
68. TorresRouff, C. Cranial vault modification and ethnicity in middle horizon San Pedro de Atacama, Chile. *Curr. Anthrop.* **43**, 163–171 (2002).
69. Torres-Rouff, C. *Shaping Identity: Cranial Vault Modification in the Pre-Columbian Andes* (University of California, 2003).
70. Gélis, J. Refaire le corps: Les déformations volontaires du corps de l'enfant à la naissance. *Ethnol. Fr.* **14**, 7–28 (1984).
71. Blom, D. E. *Tiwanaku Regional Interaction and Social Identity: a Bioarchaeological Approach* (University of Chicago, 1999).
72. De Groote, I. & Humphrey, L. T. Characterizing evulsion in the Later Stone Age Maghreb: Age, sex and effects on mastication. *Quat. Int.* **413**, 50–61. https://doi.org/10.1016/j.quaint.2015.08.082 (2016).
73. Mower, J. Deliberate ante-mortem dental modification and its implications in archaeology, ethnography and anthropology. *Pap. Inst. Archaeol.* **10**, 37–53. https://doi.org/10.5334/pia.137 (1999).
74. Blackwood, B. & Danby, P. A study of artificial cranial deformation in New Britain. *J. Anthr. Inst. Brit.* **85**, 173–191 (1955).
75. O'Loughlin, V. D. Effects of different kinds of cranial deformation on the incidence of wormian bones. *Am. J. Phys. Anthropol.* **123**, 146–155. https://doi.org/10.1002/ajpa.10304 (2004).
76. Duncan, W. N. & Hofling, C. A. Why the head? Cranial modification as protection and ensoulment among the Maya. *Ancient Mesoamer.* **22**, 199–210 (2011).
77. Rorabaugh, A. N. & Shantry, K. A. From labrets to cranial modification: credibility enhancing displays and the changing expression of Coast Salish resource commitments. *J. of Isl. Coast. Archaeol.* **12**, 380–397. https://doi.org/10.1080/15564894.2016.1203835 (2017).
78. Coneller, C. Power and society: Mesolithic Europe. In *The Oxford Handbook of the Archaeology of Death and Burial* (eds Nilsson, S. L. & Tarlow, S.) 347–358 (Oxford University Press, 2013). https://doi.org/10.1093/oxfordhb/9780199569069.013.0018.
79. Clark, G. & Neeley, M. 10. Social differentiation in European mesolithic burial data. In *Mesolithic Northwest Europe: Recent Trends* (eds Rowley-Conwy, P. A. et al.) 121–127 (Sheffield, 1987).
80. Formicola, V. From the Sunghir children to the Romito dwarf: aspects of the Upper Paleolithic funerary landscape. *Curr. Anthrop.* **48**, 446–453 (2007).
81. Nilsson Stutz, L. *Embodied Rituals and Ritualized Bodies: Tracing Ritual Practices in Late Mesolithic Burials* (Almqvist & Wiksell, 2003).
82. Pettitt, P. *The Palaeolithic Origins of Human Burial* (Routledge, 2010).
83. Binford, L. R. Mortuary practices: their study and their potential. *Mem. Soc. Am. Archaeol.* **25**, 6–29 (1971).
84. Goldstein, L. One-dimensional archaeology and multi-dimensional people: spatial organization and mortuary analysis. In *The Archaeology of Death* (eds Chapman, R. et al.) 53–49 (1981).
85. Saxe, A. A. Social dimensions of mortuary practices in a Mesolithic population from Wadi Haifa, Sudan. *Mem. Soc. Am. Archaeol.* **25**, 39–57 (1971).
86. Meiklejohn, C., Brinch Petersen, E. & Babb, J. From single graves to cemeteries: an initial look at chronology in Mesolithic burial practice. *Mesolithic Horizons* **2**, 639–649 (2009).
87. Riel-Salvatore, J. & Gravel-Miguel, C. Upper Palaeolithic mortuary practices in Eurasia: a critical look at the burial record. In *The Oxford Handbook of the Archaeology of Death and Burial* (eds Nilsson, S. L. & Tarlow, S.) 302–346 (Oxford University Press, 2013). https://doi.org/10.1093/oxfordhb/9780199569069.013.0017.
88. Guido, M. A. et al. Climate and vegetation dynamics of the Northern Apennines (Italy) during the Late Pleistocene and Holocene. *Quat. Sci. Rev.* **231**, 106206. https://doi.org/10.1016/j.quascirev.2020.106206 (2020).
89. Rellini, I., Firpo, M., Martino, G., Riel-Salvatore, J. & Maggi, R. Climate and environmental changes recognized by micromorphology in Paleolithic deposits at Arene Candide (Liguria, Italy). *Quat. Int.* **315**, 42–55. https://doi.org/10.1016/j.quaint.2013.05.050 (2013).
90. Holt, B. M. & Formicola, V. Hunters of the Ice Age: the biology of Upper Paleolithic people. *Am. J. Phys. Anthropol.* **137**, 70–99. https://doi.org/10.1002/ajpa.20950 (2008).
91. Sparacello, V. S. et al. Projectile weapon injuries in the Riparo Tagliente burial (Veneto, Italy) provide early evidence of Late Upper Paleolithic intergroup conflict. *Sci. Rep* **15**, 14857. https://doi.org/10.1038/s41598-025-94095-x (2025).
92. Kacki, S. et al. Complex mortuary dynamics in the Upper Paleolithic of the decorated Grotte de Cussac, France. *Proc. Natl. Acad. Sci. USA* **117**, 14851–14856. https://doi.org/10.1073/pnas.2005242117 (2020).
93. Formicola, V. X-linked hypophosphatemic rickets: A probable upper paleolithic case. *Am. J. Phys. Anthropol.* **98**, 403–409 (1995).
94. Formicola, V., Frayer, D. W. & Heller, J. A. Bilateral absence of the lesser trochanter in a Late Epigravettian skeleton from Arene Candide (Italy). *Am. J. Phys. Anthropol.* **83**, 425–437. https://doi.org/10.1002/ajpa.1330980403 (1990).
95. Sparacello, V. S. et al. Further insights on Late Upper Paleolithic (Epigravettian) funerary use of AreneCandide Cave (Liguria, Italy). *Am. J. Phys. Anthropol.* **68**(suppl.), 234–235 (2019).
96. Posth, C. et al. Palaeogenomics of upper palaeolithic to neolithic European hunter-gatherers. *Nature* **615**, 117–126. https://doi.org/10.1038/s41586-023-05726-0 (2023).
97. Cignoni, P. et al. MeshLab: an open-source mesh processing tool. In *Eurographics Italian chapter conference* (eds Scarano, V. et al.) 129–136 (2008).
98. Schlager, S. Morpho and Rvcg – Shape analysis. In *Statistical Shape and Deformation Analysis* (eds Zheng, G., Li, S., Székely, G. et al.) 217–256 (Academic Press, 2017).
99. Bookstein, F. L. Principal warps: Thin-plate splines and the decomposition of deformations. *IEEE Trans. Pattern Anal. Mach. Intell.* **11**, 567–585. https://doi.org/10.1109/34.24792 (1989).
100. Gunz, P., Mitteroecker, P. & Bookstein, F. L. Semilandmarks in three dimensions. In *Modern Morphometrics in Physical Anthropology* (ed. Slice, D. E.) 73–98 (Springer, 2005).
101. Bookstein, F. L. *Morphometric Tools for Landmark Data: Geometry and Biology* (Cambridge University Press, 1991).
102. Gower, J. C. Generalized procrustes analysis. *Psychometrika* **40**, 33–51. https://doi.org/10.1007/bf02291478 (1975).
103. Rohlf, F. J. & Slice, D. Extensions of the procrustes method for the optimal superimposition of landmarks. *Syst. Biol.* **39**, 40–59. https://doi.org/10.2307/2992207 (1990).
104. Pearson, K. Principal components analysis. *Lond. Edinb. Dublin Philos. Mag. J. Sci.* **6**, 559 (1901).
105. Moghimbeygi, M. & Nodehi, A. Multinomial principal component logistic regression on shape data. *J. Classif.* **39**, 578–599. https://doi.org/10.1007/s00357-022-09423-x (2022).
106. Hautavoine, H., Arnaud, J., Balzeau, A. & Mounier, A. Quantifying hominin morphological diversity at the end of the middle Pleistocene: Implications for the origin of Homo sapiens. *Am. J. Biol. Anthropol.* **184**, e24915. https://doi.org/10.1002/ajpa.24915 (2024).
107. Venables, B. & Ripley, B. *Modern Applied Statistics with S* (Springer, 2002). https://doi.org/10.1007/b97626.
108. Mitteroecker, P. & Gunz, P. Advances in geometric morphometrics. *Evol. Biol.* **36**, 235–247. https://doi.org/10.1007/s11692-009-9055-x (2009).

Acknowledgements

Research is funded by DM247 2022 MUR Italy Investment 1.2 "Funding projects presented by young researchers", grant number MCSA_0000035, project "IEPDA": Identity society and ecology of the last Upper Palaeolithic

foragers through multi-technique dental anthropology (ID). VSS has received financial support from the French State in the framework of the "Investments for the future" Program, IdEx Bordeaux, Project BUR.P.P.H., reference ANR-10-IDEX-03-02, and Fondazione di Sardegna 2022 project TRA.DIS.CO. (CUP F73C23001620007). TM is supported by project grant DiVInA (UNIFI_FSC2022) funded by Regione Toscana and Sistema Museale di Ateneo University of Florence. DF is supportend by grant project HEIMEN (PR FSE+ 2021-2027) funded by Regione Toscana and Istituto Italiano di Preistoria e Protostoria. The authors thank the Soprintendenza Archeologia Belle Arti e Paesaggio per le province di Imperia e Savona for the permission to conduct this work. For assistance during data collection and collaboration during the analysis, we thank the curators and staff of the Museo di Archeologia Ligure, Museo Archeologico del Finale, Museo di Storia Naturale dell'Università di Firenze Sezione di Antropologia e Etnologia, Museo Navale Romano di Albenga, Museo G.G. Gemmellaro dell'Università di Palermo), Dipartimento di Studi Umanistici dell'Università di Ferrara, and Museo Vittorino Cazzetta di Selva di Cadore. We are also grateful to the Unità Operativa SOS Radiologia of the Santa Maria Nuova Hospital, Firenze, for the medical 3D scanning of skeletal materials stored at the MSNF. A special thanks goes to Mario.

Author contributions

TM, ID, JMC, VSS, and AR conceptualized the study. TM, FP, and RC collected 3D models of specimens housed at the Museum of Anthropology in Florence; VSS collected 3D models of archaeological samples from Ligury, Sicily, the University of Ferrara, and Veneto. TM performed the virtual reconstruction of AC12, as well as the geometric morphometrics and data analyses. TM, ID, and AR aligned the cranial elements. TM and ID drafted the original manuscript. VSS made significant contribution to the discussion of the results, and TM, ID, AR, JMC and VSS wrote the final version of the manuscript. TM, VSS, AR, GC, DF, FS, FDV, MZ, FP, RC, MP, FF, LS, JMC, and ID reviewed and revised the manuscript. ID is the senior author of this study.

Declarations

Competing interests

The authors declare no competing interests.

Additional information

Supplementary Information The online version contains supplementary material available at https://doi.org/10.1038/s41598-025-13561-8.

Correspondence and requests for materials should be addressed to I.D.

Reprints and permissions information is available at www.nature.com/reprints.

Publisher's note Springer Nature remains neutral with regard to jurisdictional claims in published maps and institutional affiliations.